AD-A038 418 NAVAL RESEARCH LAB WASHINGTON D C F/G 20/8
USE OF AN INTRINSIC GERMANIUM DETECTOR ARRAY FOR AN AERIAL SURV--ETC(U)
FEB 77 K W MARLOW, G W PHILLIPS E(05-1)1670

UNCLASSIFIED NRL-MR-3452 NL

| OF |
AD
A038418

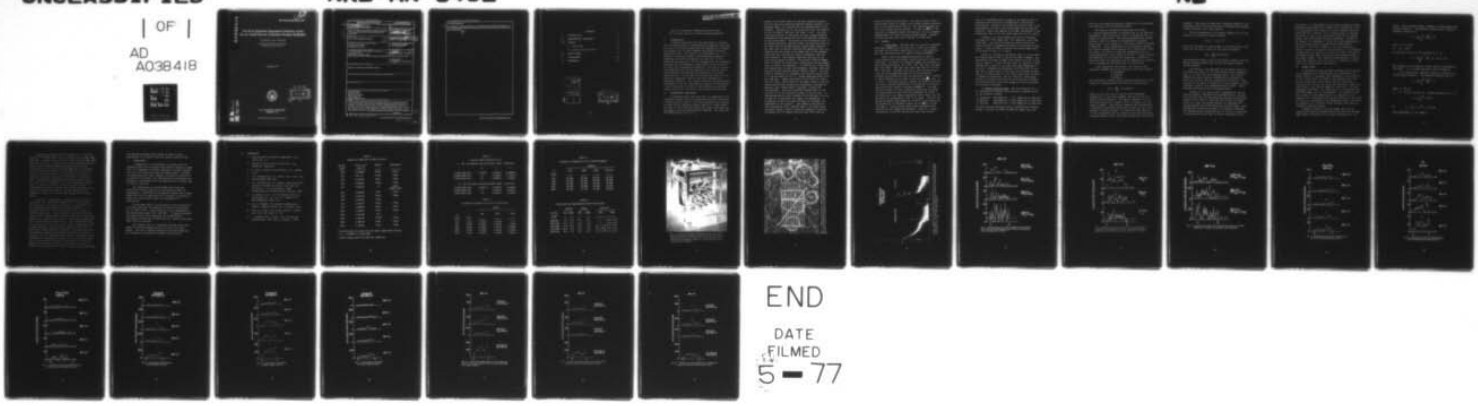

END

DATE
FILMED
5-77

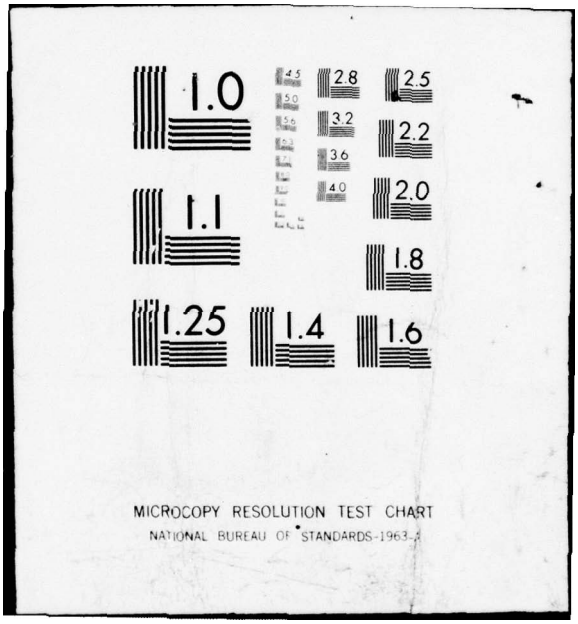
1.0
1.1
1.25
1.4
1.6
1.8
2.0
2.2
2.5
2.8
3.2
3.6
4.0
4.5
5.0
5.6
MICROCOPY RESOLUTION TEST CHART
NATIONAL BUREAU OF STANDARDS-1963-A

NRL Memorandum Report 3452

Use of an Intrinsic Germanium Detector Array for an Aerial Survey of Surface Nuclear Radiation

K. W. MARLOW AND G. W. PHILLIPS

Radiation Technology Consultant Staff
Radiation Technology Division

February 1977

NAVAL RESEARCH LABORATORY
Washington, D.C.

SECURITY CLASSIFICATION OF THIS PAGE *(When Data Entered)*

REPORT DOCUMENTATION PAGE

READ INSTRUCTIONS BEFORE COMPLETING FORM

1. REPORT NUMBER: NRL ~~Memorandum Report~~ 3452	2. GOVT ACCESSION NO.
3. RECIPIENT'S CATALOG NUMBER	
4. TITLE *(and Subtitle)*: USE OF AN INTRINSIC GERMANIUM DETECTOR ARRAY FOR AN AERIAL SURVEY OF SURFACE NUCLEAR RADIATION	5. TYPE OF REPORT & PERIOD COVERED: Final report on work performed Ma[illegible] June [illegible]76,
	6. PERFORMING ORG. REPORT NUMBER
7. AUTHOR(s): Keith W. Marlow and Gary W. Phillips	8. CONTRACT OR GRANT NUMBER(s): ERDA letter agreement AE(05-1)-1670 of 9 January 1970
9. PERFORMING ORGANIZATION NAME AND ADDRESS: Naval Research Laboratory, Washington, D.C. 20375	10. PROGRAM ELEMENT, PROJECT, TASK AREA & WORK UNIT NUMBERS: NRL Problem H01-48B
11. CONTROLLING OFFICE NAME AND ADDRESS: U.S. Energy Research and Development Administration, Grand Junction Office, Grand Junction, Colorado 81501	12. REPORT DATE: February 1977 (12 33p.)
	13. NUMBER OF PAGES: 32
14. MONITORING AGENCY NAME & ADDRESS *(if different from Controlling Office)*	15. SECURITY CLASS. *(of this report)*: UNCLASSIFIED
	15a. DECLASSIFICATION/DOWNGRADING SCHEDULE

16. DISTRIBUTION STATEMENT *(of this Report)*

Approved for public release; distribution unlimited.

17. DISTRIBUTION STATEMENT *(of the abstract entered in Block 20, if different from Report)*

18. SUPPLEMENTARY NOTES

19. KEY WORDS *(Continue on reverse side if necessary and identify by block number)*

Intrinsic germanium
Gamma ray detector
Nuclear instrumentation
Natural radioactivity
Airborne nuclear detectors

20. ABSTRACT *(Continue on reverse side if necessary and identify by block number)*

This report describes the results of an experiment to measure the natural gamma radiation emitted from the earth's surface with the aid of radiation detectors mounted in an aircraft. For comparison, two detector systems were used: an array of intrinsic germanium detectors with a total active volume of 0.4 liter and a single NaI(Tℓ) scintillation detector 30.5 cm diam × 30.5 cm long. Data were recorded on flights at altitudes of 60, 120, 240, 300 and 5100 meters and with average airspeed of 200 knots. The results are presented and compared. A discussion is presented

(Continues) → next page

DD FORM 1 JAN 73 1473 EDITION OF 1 NOV 65 IS OBSOLETE S/N 0102-014-6601

SECURITY CLASSIFICATION OF THIS PAGE *(When Data Entered)*

251 950

20. Abstract (Continued)

cont.

on the application of germanium detectors to the atmospheric radon problem; in particular, on the use of the photons with energy 295, 352 and 609 keV to determine the respective contributions from the air and the surface.

CONTENTS

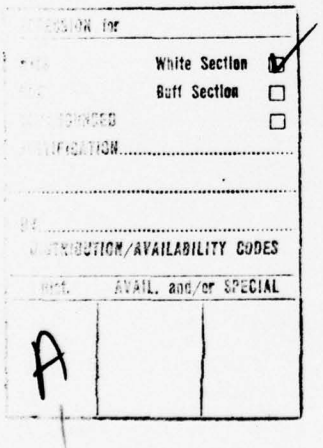

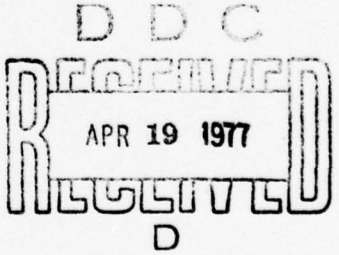

Use of an Intrinsic Germanium Detector Array for an Aerial Survey of Surface Nuclear Radiation

I. INTRODUCTION

A limited experiment has been undertaken to investigate the desirability of high-resolution gamma-ray detectors for use in the aerial prospecting for uranium and to compare the results with the more commonly used NaI(Tℓ) scintillation detectors. The goals of the experiment are: (1) to attempt to determine whether high-resolution germanium gamma-ray detectors are superior (in practice) to the scintillation detectors, and (2) assuming that the germanium detectors are advantageous, suggest what the detector size or other related parameters should be. An array of intrinsic germanium detectors was operated in an aircraft over a test area which had already been surveyed by a scintillation system. A large NaI(Tℓ) detector was flown with the array for comparison, and the data were recorded for subsequent analysis. This report describes the experimental conditions of the test and presents results of the analysis. A brief discussion is given on the evaluation of airborne radon activity with the aid of high-resolution detectors.

II. EXPERIMENTAL CONDITIONS

A prototype array[1] was used (Fig. 1) consisting of 12 closed-end coaxial intrinsic germanium detectors, each with a frontal area of about 15 cm^2 and an average active volume of about 36 ml, providing greater than 0.4 l total volume. The cost of this array and associated signal processing and recording system was approximately $180,000. The array was

Note: Manuscript submitted February 1, 1977.

mounted in the rear cabin of a P3 Navy research aircraft with the detectors pointing downward looking through a 1/2" aluminum plate, 3/4" plywood and the aluminum body of the airplane. Mounted next to the array was a 30.5 cm diameter by 30.5 cm NaI(Tℓ) detector (12" diam. x 12"). The data from each detector in the array was sent through separate preamplifiers and amplifiers into a multiplexer[2] operated in anti-coincidence. The output of the multiplexer went to an analog-to-digital converter (ADC) and then was stored in the lower half of an 8192 channel pulse-height analyzer. The data from the NaI(Tℓ) detector was amplified, sent to a separate ADC and routed to the upper half of the analyzer. After each run the data was stored on magnetic tape for later analysis. The signals from each detector in the array were aligned by using a ^{60}Co source (1332 keV gamma-rays) to adjust the gains and a ^{241}Am source (60 keV gamma-rays) to adjust the baselines. A 70 Km (44 mi) flight path was cleared over an area near Richmond, Virginia, which had previously been surveyed using a NaI(Tℓ) array.[3] The path flown is indicated by a diagonal line between points C and D on the map shown in Fig. 2. Ground speed was about 47 m/sec (220 mph). Passes were made at 60 m (200 ft), 120 m (400 ft) twice, 240 m (800 ft), and 300 m (1000 ft) and 32 second spectra were alternately accumulated, recorded on magnetic tape (taking about 4 seconds), cleared and reaccumulated. Thus each spectrum covered about 3.1 Km (2.0 mi) out of an interval of about 3.5 Km (2.2 mi). A 1024-second spectrum was recorded at an altitude of 5.2 Km (17,000 ft) to determine the cosmic ray background. A preliminary flight over water was made to determine the background in the aircraft. Also shown on the map is a grid (horizontal lines) showing some of the lines flown previously using a NaI(Tℓ) array and regions of activity determined for ^{40}K (dashed outline) and ^{208}Tℓ from the

decay of thorium (solid line).[3] The data of Foote[3] show a well-defined region of higher than average thorium concentration in the area shown in Fig. 2. The indicated region for ^{40}K is not nearly so well defined. In that region the ^{40}K intensity is somewhat higher than average, but in a somewhat random manner with high and low intensity areas. Sporadic activity was also seen from ^{214}Bi due to ^{226}Ra decay.

III. RESULTS

A. Array Data. The data from the intrinsic germanium array were summed for each pass (Fig. 3 shows the summed spectrum for the 200 ft pass from C to D). This spectrum was then analyzed using the computer Program HYPERMET.[4]

Table 1 gives the gamma-rays observed at 200 ft, their intensities, their parent nuclei, and their long-lived precursors. Of these, the following gamma rays appeared to have useful activities, for ^{232}Th: 238, 583, 911, and 2615 keV; for ^{226}Ra: 295, 352, 609, 1120, and 1764 keV; and for ^{40}K: 1461 keV. Analyses were run on each 32-second spectrum for these gamma rays plus 511 keV from positron annihilation and 662 keV from the ubiquitous ^{137}Cs. Results of these analyses for the 200 ft data are shown in Figs. 4, 5, and 6. (To obtain accurate results for data with so very few counts required modification of the method of calculating statistical weights in Program HYPERMET.[5]) The peak counts are shown for each consecutive 32-second run along the track between C and D and the background at 17,000 ft is indicated by the dashed horizontal lines, except for 511 keV where the background at 1000 ft is shown. (The 511 keV counts increased considerably at 17,000 ft to 60 counts per 32 seconds due to increased cosmic ray intensity at high altitudes.) Counts significantly above background were observed for all gamma rays analyzed. There is a strong correlation in the 2615 and 911 keV data from thorium

(Fig. 4), confirming that the peak in the data is due to thorium activity and not to background or statistical fluctuations. Moreover the strong ^{40}K activity (Fig. 5) is uncorrelated with any of the other gamma rays as might be expected. There also appears to be some correlation in the radium data (Fig. 6) at the broad hump just left of center.

Figures 7, 8, and 9 compare the data at different altitudes for ^{232}Th (2615 keV), ^{40}K (1461 keV), and ^{226}Ra (1120 keV). The data are aligned at point D which was better defined by landmarks and seems to track better than point C. Thus the 200 ft data are the mirror image plots of the data in Figs. 4, 5, and 6.

There is a distinct correlation (Fig. 7) in the 2615 keV thorium peak at 200 ft and the two 400 ft passes. The correlation is weaker at 800 ft and there is little if any left at 1000 ft. In the ^{40}K data (Fig. 8) there is a clear correlation at least in the rise from near background at the left. Although the statistics for ^{226}Ra (Fig. 9) are poor due to weak activity there may still be some correlation in the broad hump, in this figure just right of center. It should be pointed out that the track on a given pass between C and D may have been off by as much as 1.5 miles; this could result in different apparent activity profiles for different altitudes.

B. NaI(Tℓ) Detector Data. The data from the 12" x 12" diam NaI(Tℓ) detector were analyzed by summing counts in the following windows:

1) Potassium, 1340-1560 keV (^{40}K gamma ray at 1461 keV)
2) Uranium, 1650-1890 keV (^{214}Bi gamma ray at 1764 keV)
3) Thorium, 2470-2750 keV ($^{208}Tℓ$ gamma ray at 2615 keV)

The data were also analyzed using a 1650-2470 keV uranium window to include the 2204 and 2438 keV gamma rays from

^{214}Bi but with less satisfactory results due to interference from thorium as will be discussed below.

Two separate background subtractions were made, 1) a system background due to radioactivity in the detectors, instruments, and the aircraft, and 2) a background due to cosmic-ray interactions. The system background was assumed constant, while the cosmic-ray background was assumed proportional to the counts in a high-energy window from 5350 to 6690 keV. These backgrounds in the potassium, uranium and thorium windows were determined by a low-altitude flight over water, for which the data was predominantly due to system background, and a flight at 17,000 ft, where the data was dominated by the cosmic-ray background. Analysis of these data gave two equations with two unknowns to be solved for the background from each source in each window.

After background subtraction, the counts in each window are assumed due to one or more of the three sources:

1) Potassium
2) Uranium
3) Thorium

The relationship between source strength and counts in each window of the spectrum can be written in matrix form[6]

$$N(I) = \sum_{J} A(I,J) \cdot S(J)$$

where the $N(I)$ are the net counts (after background subtraction) in the three windows, and the $S(J)$ are the unknown source strengths. The matrix elements $A(I,J)$ are the counts expected in window I due to a source J of unit source strength. These matrix elements were determined by a laboratory calibration using point sources of the three elements of known strength. It would have been better to do this calibration with the system on the plane and using extended sources rather than point sources but this was not

feasible. Thus there is some error (hopefully small) in the calibrated values of A(I,J) which can introduce interferences between sources in the final results.

After determination of the matrix elements A(I,J) this matrix can be inverted to give a matrix

$$B(I,J) = [A(I,J)]^{-1}$$

Given the net counts in each window in the data spectra this matrix can be used to solve for the source strenghts

$$S(I) = \sum_{I} B(I,J) \cdot N(J)$$

The calibrated values of B(I,J) are given in Table 2 for the smaller uranium window (top) and for the larger uranium window (bottom).

The results of the analysis for the NaI(Tℓ) detector are plotted in Figs. 10, 11, and 12 which can be compared to Figs. 7, 8, and 9 for the germanium array. The features observed are quite similar, although the statistics are better in the data from the single NaI(Tℓ) detector. Thus, strictly on the basis of sensitivity, there appears to be no advantage in going to a germanium detector array. (Other possible advantages will be discussed below.)

Figures 13, 14, and 15 show a comparison of the two uranium windows, 1650-1890 keV and 1650-2470 keV, plotted with the data from the corresponding thorium and potassium windows for the 200 ft flight and the two 400 ft flights. There is a large correlation between the 1650-2470 keV uranium window and the 2470-2750 keV thorium window. This correlation is reduced in going to the smaller 1650-1890 keV uranium window, indicating that it is due in large part to interference rather than to actual coincidence of the

two sources. A calibration of the system in place and using extended sources might have reduced this interference, which is so pronounced here because the actual uranium counts are relatively low. However, for a stronger source of uranium, one should be able to get sufficient counts in the smaller window, and interference should be negligible. Because of the danger of interference, it does not seem advantageous to use the larger window in analyzing data from NaI(Tℓ) detectors. Note that in Table 2, the cross term B(2,3) (which is negative to account for interference) is increased in magnitude by a factor of 2, while the direct term B(2,2) decreases by about 40%, in going from the smaller window to the larger window. This indicates a 40% increase in sensitivity for uranium, but at the cost of a doubling in magnitude of the interference from thorium.

IV. RADON CLOUDS

A problem which has continued to plague aerial surveys is the possibility of interference due to emissions from radon "clouds" or unusually high atmospheric concentrations of the 3.8 day half-life ^{222}Rn in the uranium decay chain. The air attenuation coefficients differ by more than a factor of two from the low-energy 295 and 352 keV gamma rays from ^{214}Pb to the 1764 keV gamma ray from ^{214}Bi. All are descended from ^{222}Rn. The attenuations of the 609 and 1120 keV ^{214}Bi gamma rays are intermediate. The detected intensity ratios of these gamma rays is an indication of the amount of air attenuation and thus the distance of the source. If there is a contribution from atmospheric radon, this will be revealed by an effective source distance less than the aircraft-to-ground distance.

Although statistics on these gamma rays with the present data from the germanium array are poor, we can make some rough calculations of the expected magnitude of the

effect. For a surface source, consider a uniform plane with a source density σ. The observed intensity for a detector located at height H is

$$I_1 = \frac{\sigma}{4\pi} \int_H^\infty \frac{e^{-\mu r}}{r^2} \, dA$$

where $A = \pi(r^2 - H^2)$

or $dA = 2\pi r dr$

so that with a shift of the variable to $x = \mu r$

$$I_1 = \frac{\sigma}{2} \int_{\mu H}^\infty \frac{e^{-x}}{x} \, dx = \frac{\sigma}{2} \, E_1 \, (\mu H)$$

The integral E_1 is tabulated in most tables of mathematical functions.[7] I_1 of course approaches zero for large H.

For a radon cloud, consider a sphere of radius R with uniform source density ρ; the observed intensity will be

$$I_2 = \frac{\rho}{4\pi} \int_o^R \frac{e^{-\mu r}}{r^2} \, dV$$

where $V = \frac{4}{3} \pi r^3$

or $dV = 4\pi r^2 dr$ so that the integral becomes for $x = \mu r$

$$I_2 = \frac{\rho}{\mu} \int_o^{\mu R} e^{-x} \, dx$$

or $$I_2 = \frac{\rho}{\mu} \left[1 - e^{-\mu R}\right] \equiv \rho \, F_2 \, (\mu R)$$

which approaches ρ/μ for large R.

Tabulated in Table 3 are the values[8] of μ for an air density of 0.001293 g/cm^3 and the values[7] of E_1 at 60m, 120m, and 240m. In Table 4 are given the values of F_2 at 60m, 120m, 240m, and infinity. Table 5 gives the calculated detection ratios using tabulated gamma-ray emission ratios[9] and efficiencies for the detector array measured in the laboratory with calibrated sources; also shown are the observed ratios at 200 and 400 feet. The differences between the plane and the sphere are large at 60m and even greater at 120m. Although the experimental uncertainties are large, the data are more consistent with the uniform plane assumption. To obtain sufficient counts for a more certain discrimination between airborne and surface radiation would require at least four times the present amount of data implying an array with a larger area and/or slower flight speed.

There may be advantages in employing only the lower energy 295, 351 and 609 keV gamma rays for this purpose. One would then not require the depth of the detectors used in the present array because the stopping power of germanium is greater for these energies than for 1120 and 1764 keV gamma rays. Using shallower detectors could also increase the signal-to-noise ratio by reducing the high background due to Compton scattering of higher energy gamma rays which is basically a volume effect. This would also result in a savings in the cost of the high-purity germanium needed to make the array, or alternately a larger array could be made from the same amount of material. The fabrication cost for shallower planar or semi-planar detectors may also be less than for the coaxial detectors used in the present array. Although air attenuation is higher for the low-energy gamma rays, the detection efficiency is also higher, so that it appears there would be little if any penalty in going to a system which concentrates on detecting lower-energy gamma rays.

The optimum thickness which should be used for this application is a subject which may require further study.

V. CONCLUSIONS

A comparison of the analysis of the data from the germanium array and the single large NaI(Tℓ) detector, shows that it is possible to observe significant surface features even with this relatively small prototype array. Although the germanium array cannot compete with NaI(Tℓ) strictly on the basis of efficiency, the high-resolution eliminates the problem of interference that was observed with the data from the NaI(Tℓ) detector.

The observation of several gamma rays from both uranium and thorium sources with the array can also be advantageous. Observing the correlation between two or more gamma rays from the same source can increase the signal-to-noise ratio and further reduce any possibility of interference.

As discussed above, the difference in air attenuation with energy may also be exploited to reduce uncertainties due to radon clouds. This difference is most pronounced in the lower-energy range (295 - 609 keV). It appears possible that detectors could be optimized for simultaneously determining surface and airborne activity, however additional study would be required.

The ultimate cost of a germanium detector array will depend on detector design and on the size of the array needed. The latter depends strongly on aircraft speed and the frequency of data points required per line mile.

VI. REFERENCES

1. Manufactured by Princeton Gamma-Tech, Inc., Princeton, N.J.

2. Manufactured by Northern Scientific, Inc., Middleton, Wisconsin.

3. R. Foote, Geodata International, Inc., Dallas, Texas.

4. G.W. Phillips and K.W. Marlow, Nucl. Instr. and Methods 137 (1976) 525.

5. G.W. Phillips and K.W. Marlow, "Peak Search and Analysis of Gamma Ray Spectra with Very Low Statistics," to be published in IEEE Transactions in Nuclear Science, February 1977.

6. L. Løvberg et al., in "The Natural Radiation Environment II," ed. by J.A.S. Adams et al., CONF-720805-P1 (1972) 155.

7. See for example "CRC Standard Mathematical Tables," Chemical Rubber Co., Cleveland, Ohio.

8. From A.E. Evans, "The Atomic Nucleus," McGraw Hill, New York (1955) p. 713.

9. G. Erdtmann and W. Soyka, "Die γ-Linien der Radionuklide," KFA, Jülich, Germany, (1974).

Table 1

Gamma-rays Observed at 60m Altitude

Energy (keV)	Count rate† (sec^{-1})	Parent	Precursors
238	0.419±68	^{212}Pb	^{232}Th
295	0.22 ±9	^{214}Pb	^{226}Ra
339	0.118±59	^{228}Ac	^{232}Th
352	0.368±62	^{214}Pb	^{226}Ra
511	0.251±35	e^{+}	^{232}Th cosmic rays
583	0.162±28	^{208}Tl	^{232}Th
609	0.216±32	^{214}Bi	^{226}Ra
662	0.226±33	^{137}Cs	-
911	0.133±24	^{228}Ac	^{232}Th
969	0.068±21	^{228}Ac	^{232}Th
1120	0.108±23	^{214}Bi	^{226}Ra
1461	0.557±28	^{40}K	-
1593	0.048±14	^{208}Tl*	^{232}Th
1764	0.056±12	^{214}Bi	^{226}Ra
2615	0.146±12	^{208}Tl	^{232}Th

†uncertainties are given for the least significant digits, i.e., 0.419±68 = 0.419±0.068

*double escape peak from 2615 keV gamma ray

Table 2

Inverse Source Matrix B(I,J)

A. For the Smaller Uranium Window (1650 - 1890 keV)

	K	U	T
K(1340-1560 keV)	6.615E-2	-3.882E-2	-6.426E-3
U(1650-1890 keV)	0.0	6.555E-3	-1.375E-3
T(2470-2750 keV)	0.0	-6.066E-5	1.608E-3

B. For the Larger Uranium Window (1650 - 2470 keV)

K(1340-1560 keV)	5.615E-2	-2.744E-2	2.329E-3
U(1650-2470 keV)	0.0	4.633E-3	-2.853E-3
T(2470-2750 keV)	0.0	-4.287E-5	1.622E-3

Table 3

Intensity Integrals E_1 for a Uniform Plane

E_γ (keV)	μ (m^{-1})	Height 60m	120m	480m
295	0.043	0.02246	0.00095	0.0
352	0.034	0.04638	0.00344	0.00003
609	0.023	0.12010	0.01779	0.00063
1120	0.019	0.17500	0.03344	0.00193
1764	0.017	0.21270	0.04638	0.00344

Table 4

Intensity Integrals F_2 for a Uniform Sphere

E_γ (keV)	Radius			
	60m	120m	480m	Infinite
295	21.494	23.122	23.255	23.256
352	25.587	28.914	29.403	29.412
609	32.540	40.726	43.304	43.478
1120	35.799	47.248	52.081	52.632
1764	37.612	51.175	57.829	58.824

Table 5

Calculated and Experimental Detection Ratios

$E_{\gamma 1}/E_{\gamma 2}$ (keV)	Sphere		Plane		Observed	
	60m	120m	60m	120m	60m	120m
295/609	1.4	1.2	0.4	0.1	--	0.9 ± 0.8
295/1120	8.4	6.7	1.8	0.4	--	1.0 ± 0.8
352/1120	9.8	8.1	3.5	1.4	3.5 ± 1.8	4.3 ± 4.4
352/1764	10.9	9.0	3.5	1.2	9.1 ± 6.0	4.3 ± 4.4
609/1120	6.0	5.7	4.5	3.4	1.3 ± 0.8	1.1 ± 0.9

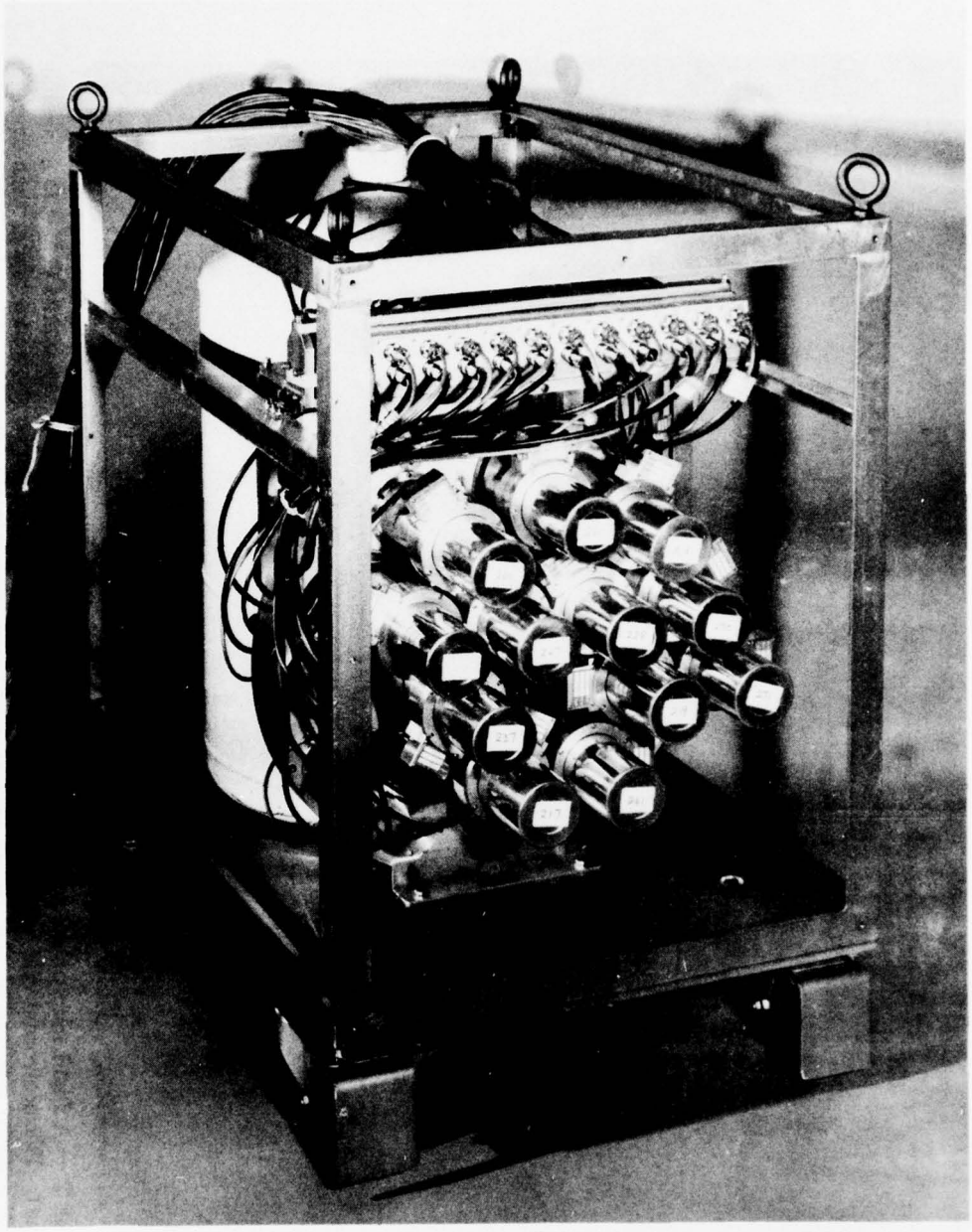

Fig. 1 — The array of 12 intrinsic germanium detectors is shown facing forward, each detector is attached to a large copper cold plate which is connected to the dewar by a copper rod. The preamps are mounted above the detectors and signal cables run to separate amplifiers, then to an anticoincidence multiplexer.

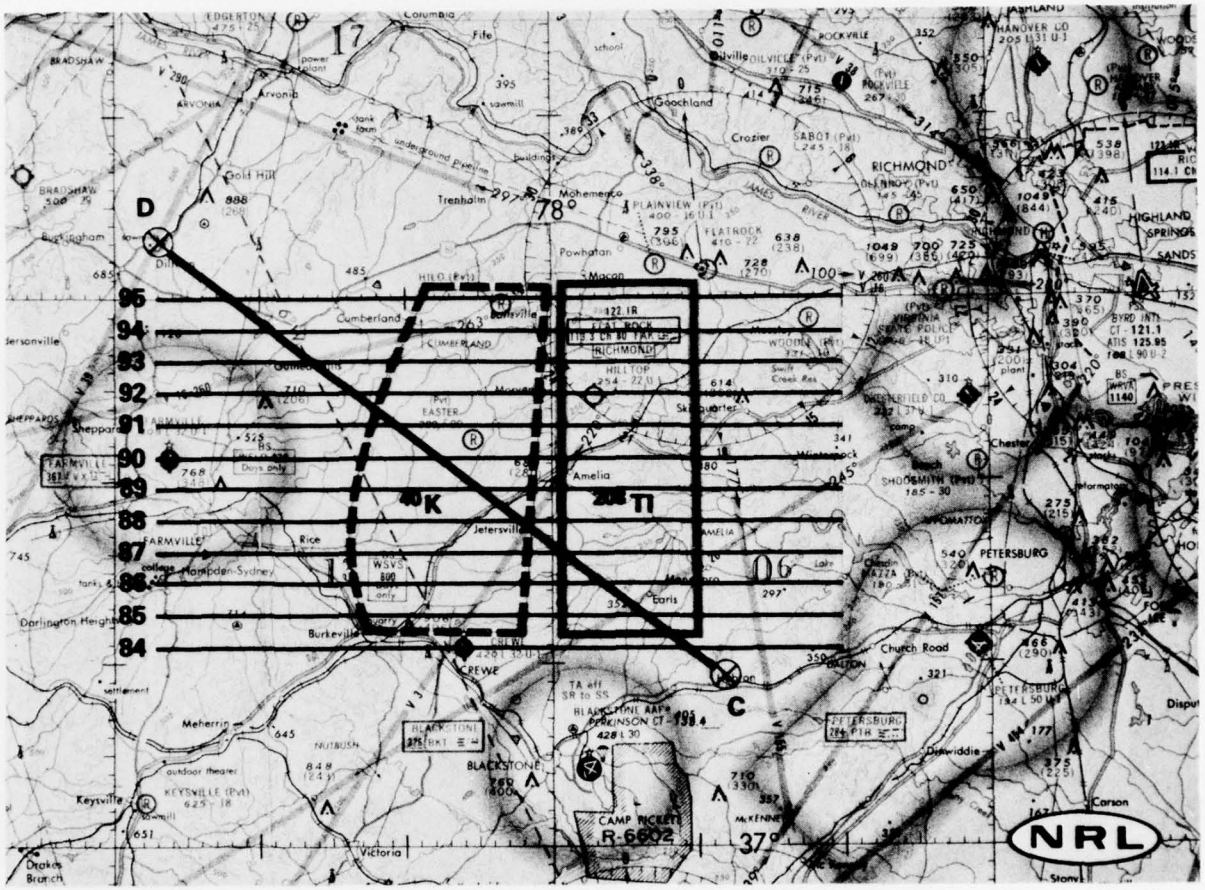

Fig. 2 — A flight map of the test area. Multiple passes were flown between points C and D (diagonal line). The horizontal grid was flown on the Geodata NaI survey, which showed a higher than average ^{40}K activity, outlined by the dashed line, and $^{208}T\ell$ activity from thorium decay outlined by the solid line.

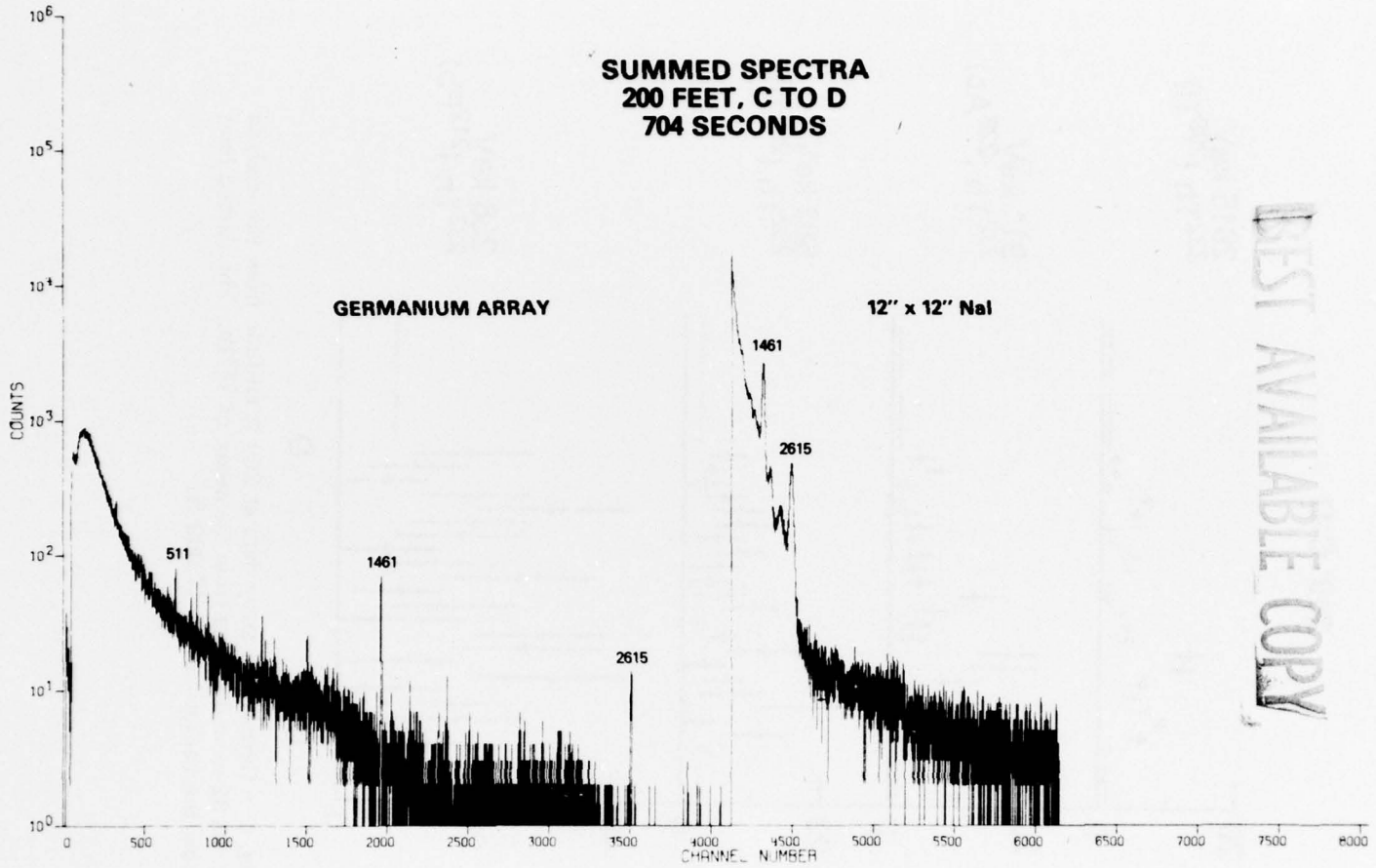

Fig. 3 — Sum spectra of 22 individual 32-second spectra taken on the pass from C to D (Fig. 2) at 200 ft altitude. The array data is on the left, and on the right is the data recorded simultaneously using a 12-in. diam × 12-in. NaI(Tℓ) detector.

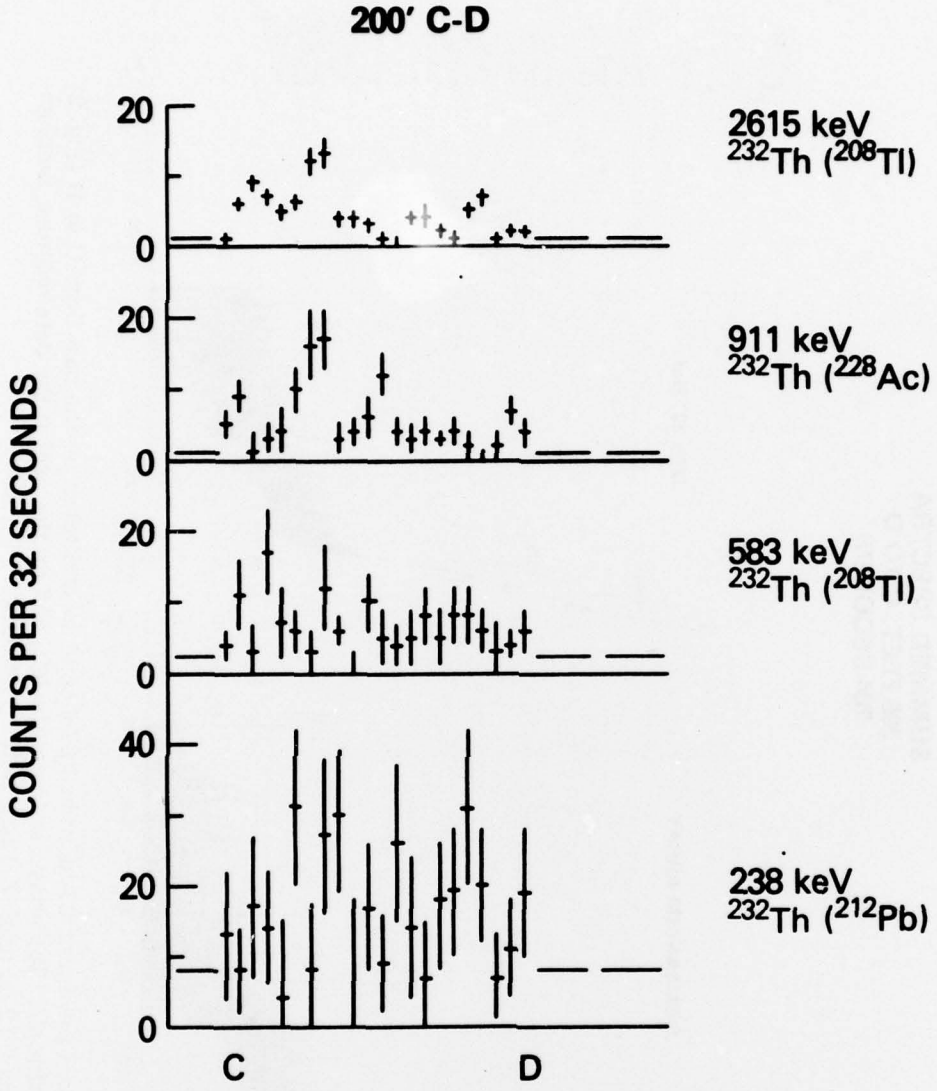

Fig. 4 — Germanium array data at 200 ft altitude from the analysis of the 32-second spectra from the decay of ^{232}Th. The dashed lines show the background at 17,000 ft.

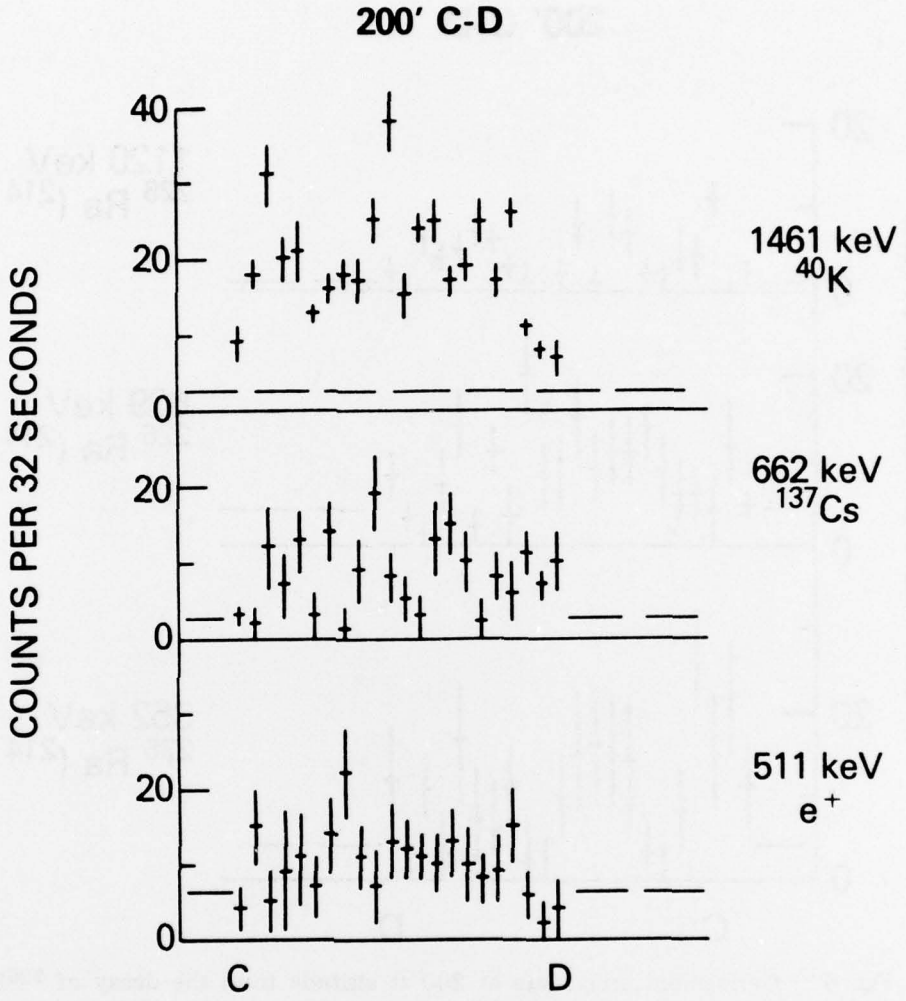

Fig. 5 — Germanium array data for ^{40}K and ^{137}Cs decay and positron annihilation (511 keV) at 200 ft altitude. Backgrounds indicated by dashed lines are at 17,000 ft except for 511 keV which is at 1000 ft.

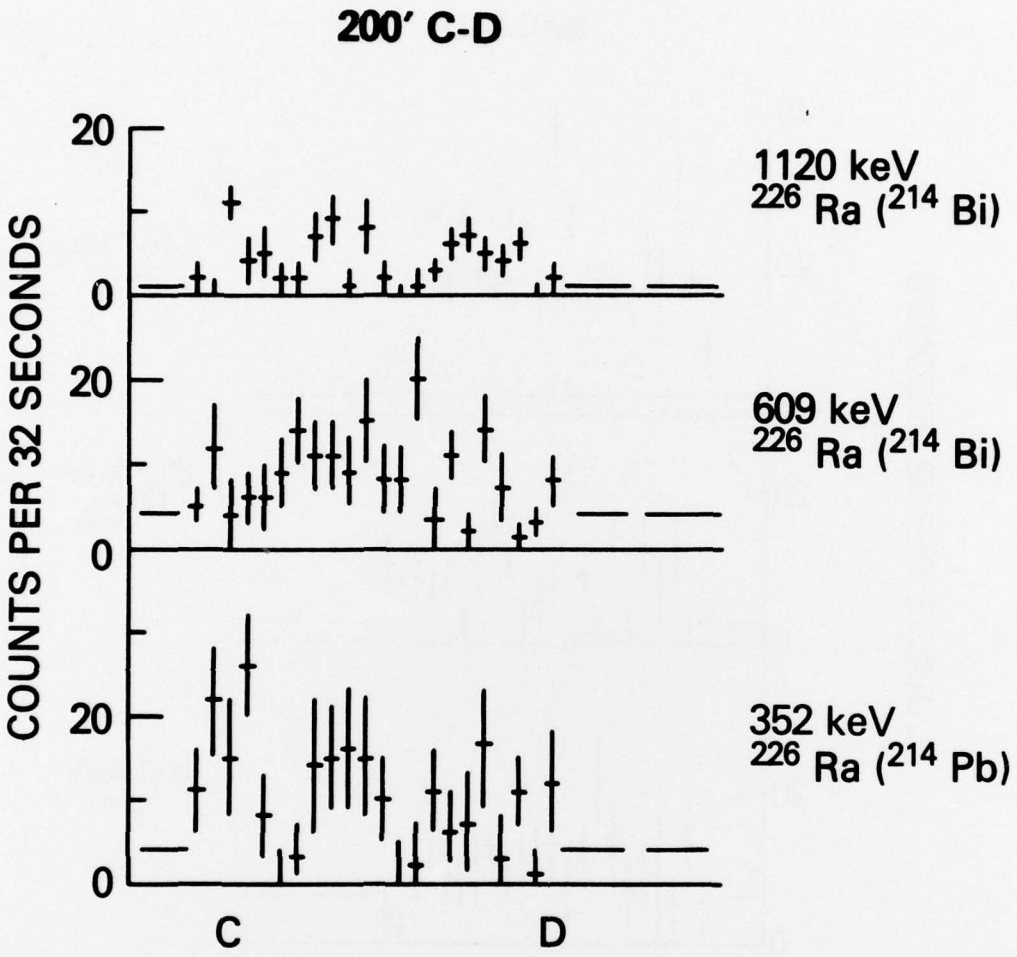

Fig. 6 — Germanium array data at 200 ft altitude from the decay of ^{226}Ra. Backgrounds at 17,000 ft are indicated by the dashed lines.

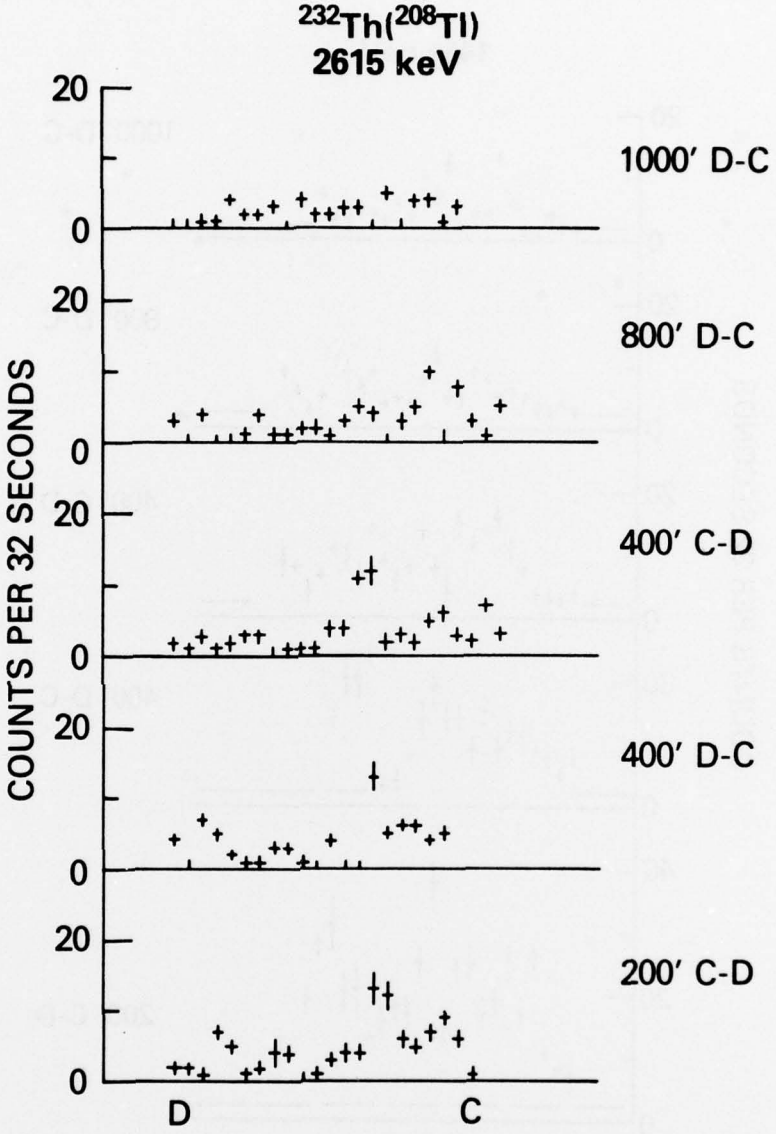

Fig. 7 — Germanium array data at all altitudes for the 2615 keV thorium peak, aligned at point D

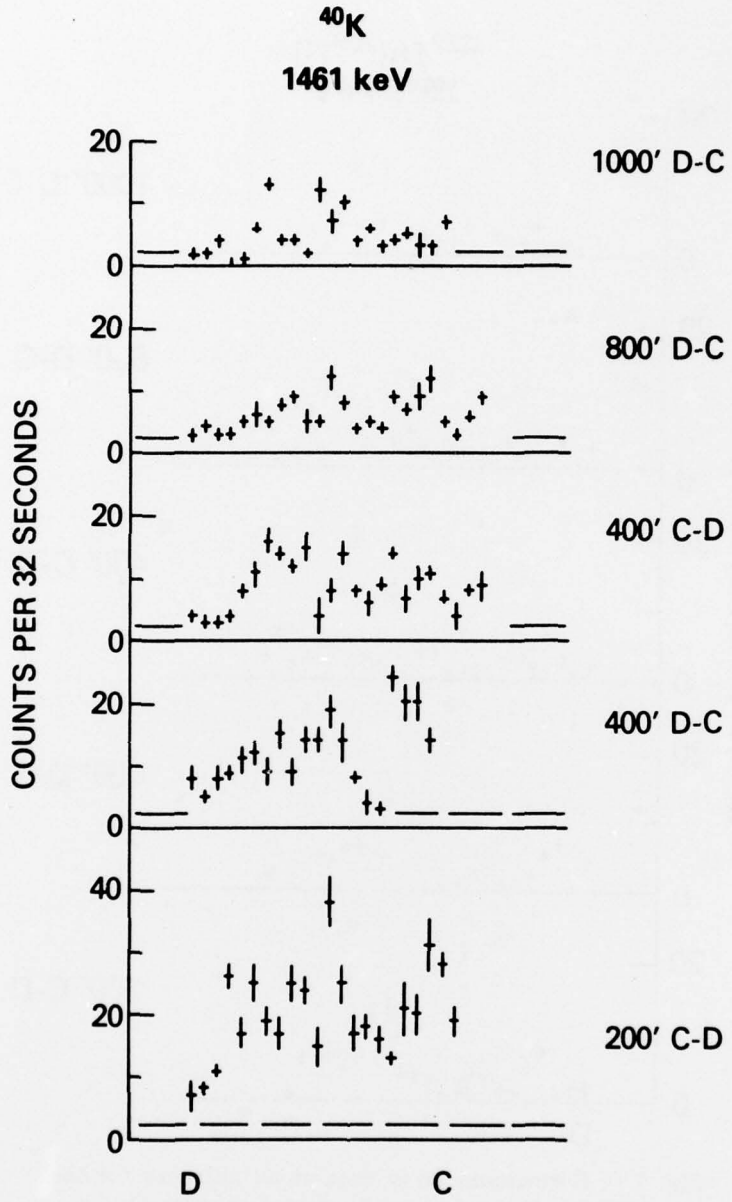

Fig. 8 — Germanium array data at all altitudes for the 1461 keV potassium peak, aligned at point D

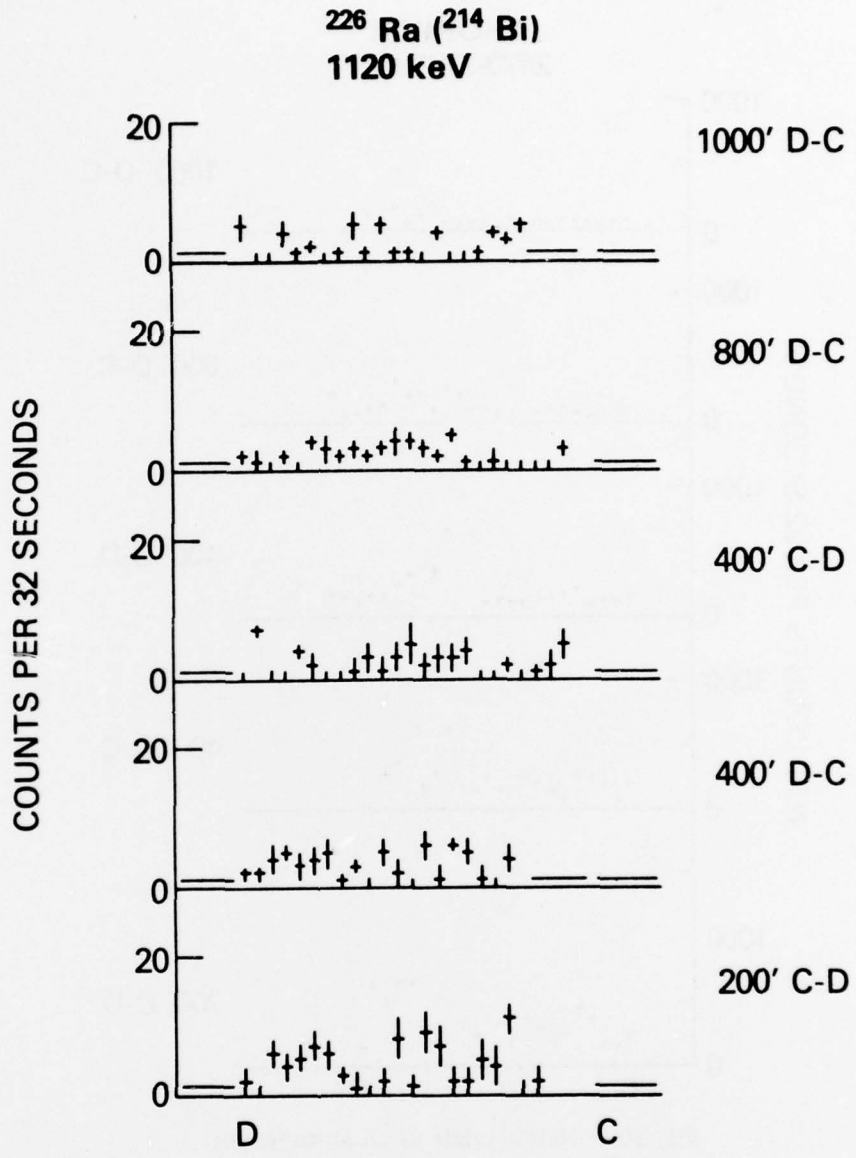

Fig. 9 — Germanium array data at all altitudes for the 1120 keV radium peak, aligned at point D

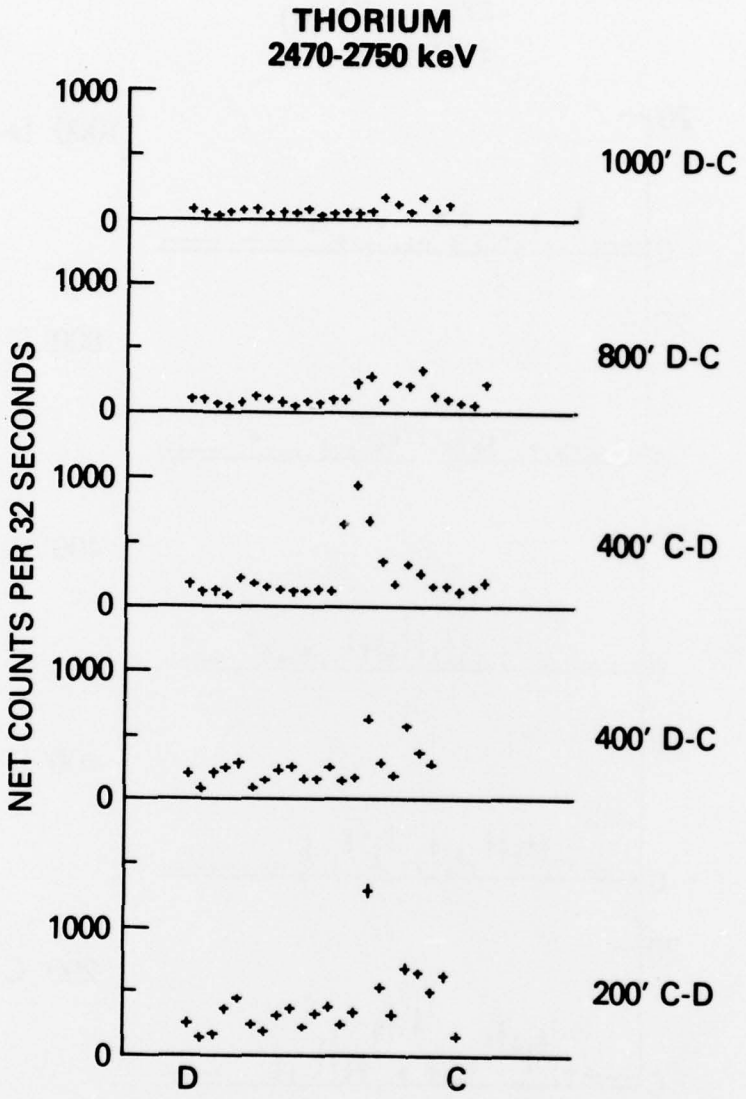

Fig. 10 — NaI(Tℓ) data at all altitudes for thorium, aligned at point D

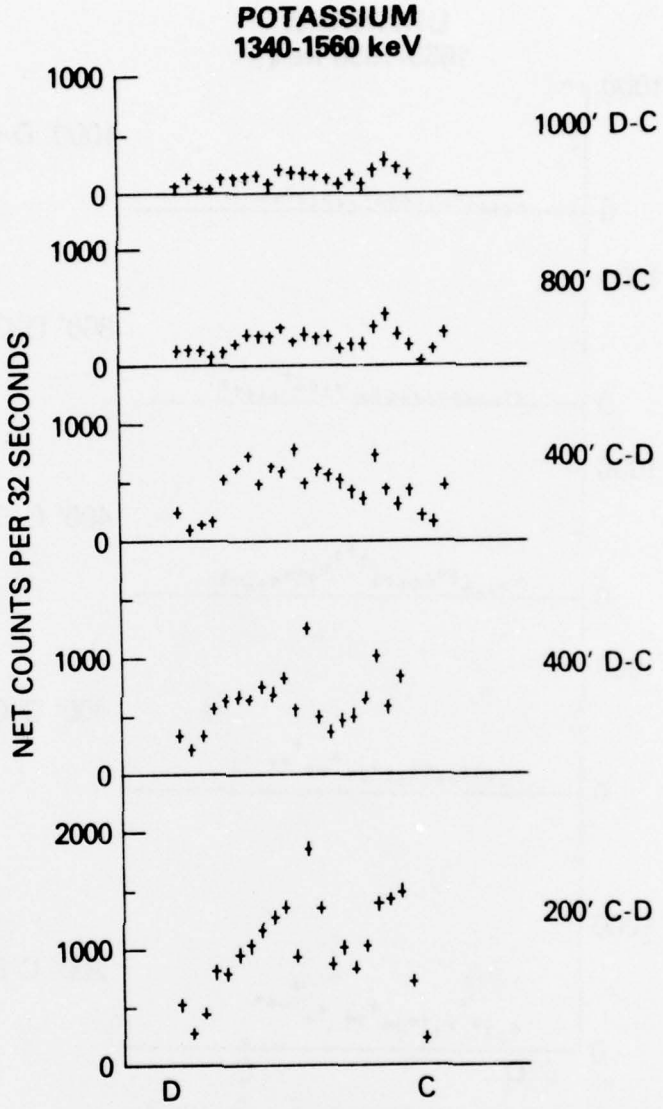

Fig. 11 — NaI(Tℓ) data at all altitudes for potassium, aligned at point D

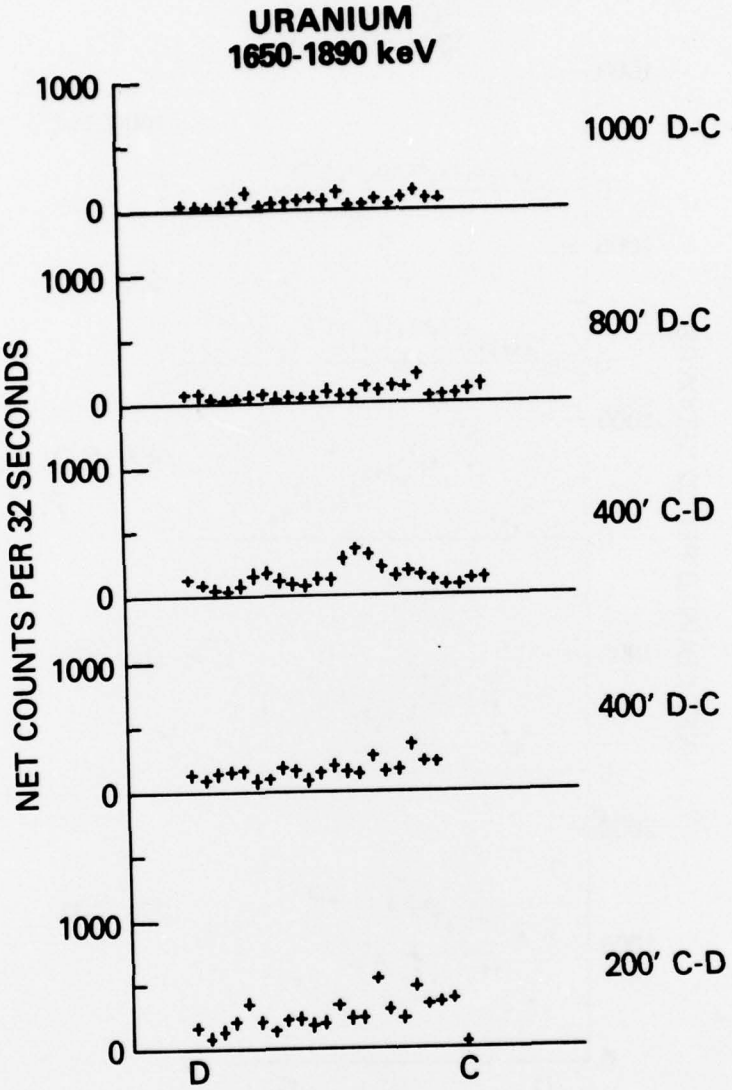

Fig. 12 — NaI(Tℓ) data at all altitudes for uranium, aligned at point D

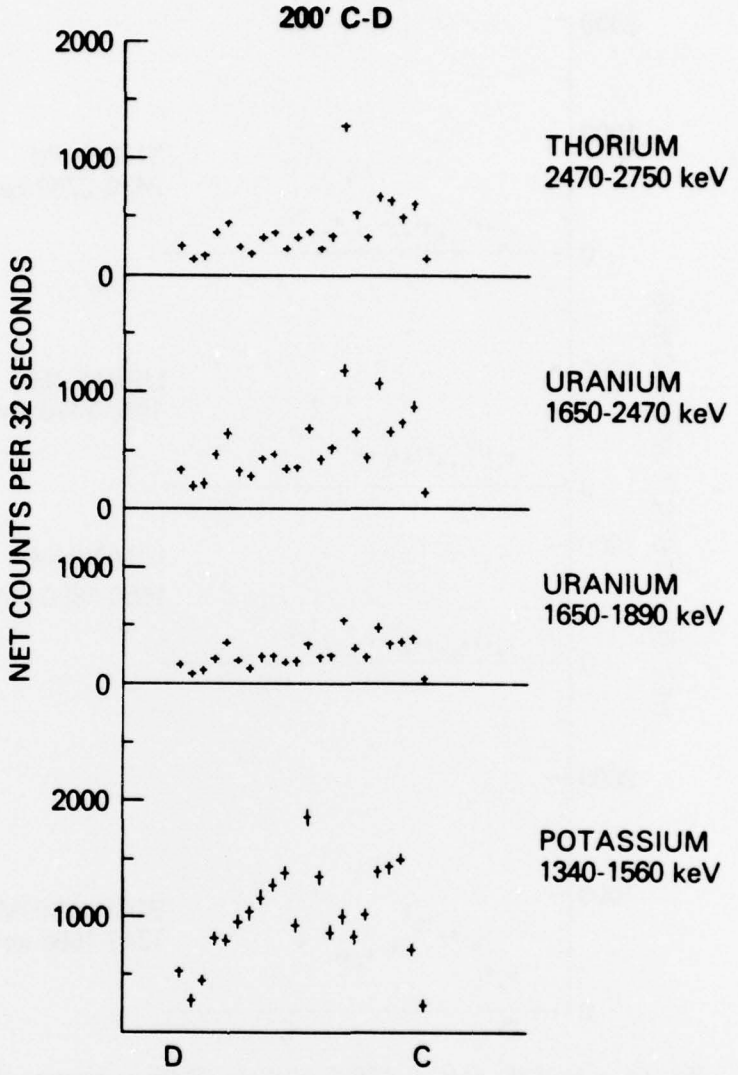

Fig. 13 — NaI(Tℓ) data at 200 ft altitude (C-D) comparing the results for the large (1650-2470 keV) and small (1650-1890 keV) uranium windows

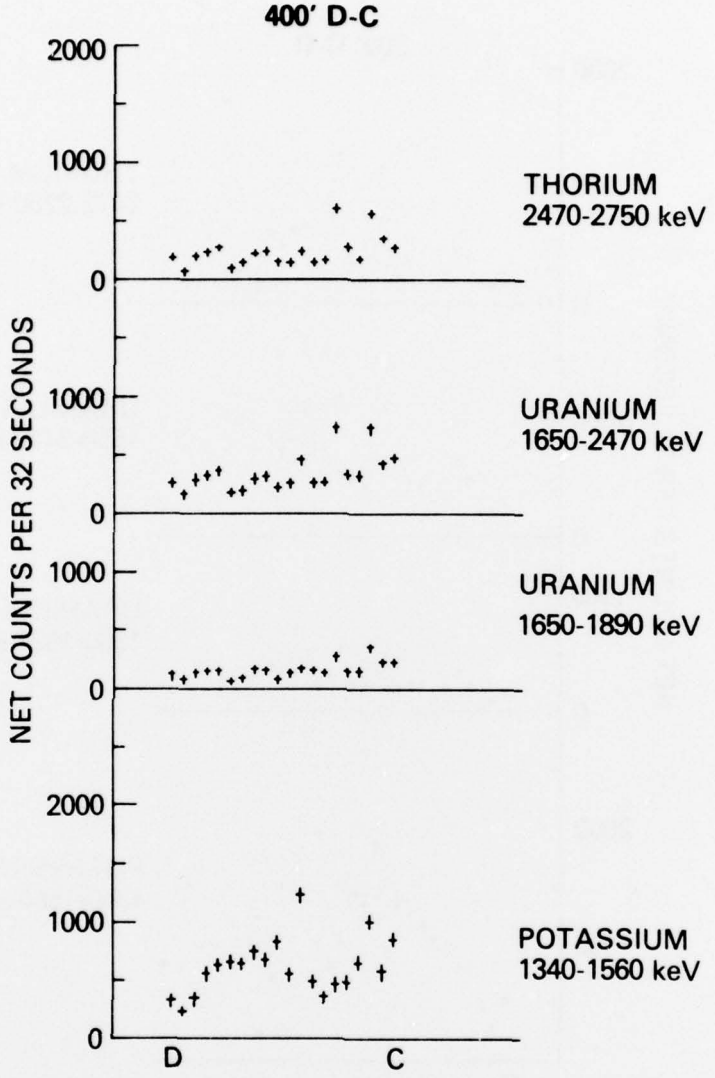

Fig. 14 — NaI(Tℓ) data at 400 ft altitude (D-C) comparing the results for the large and small uranium windows

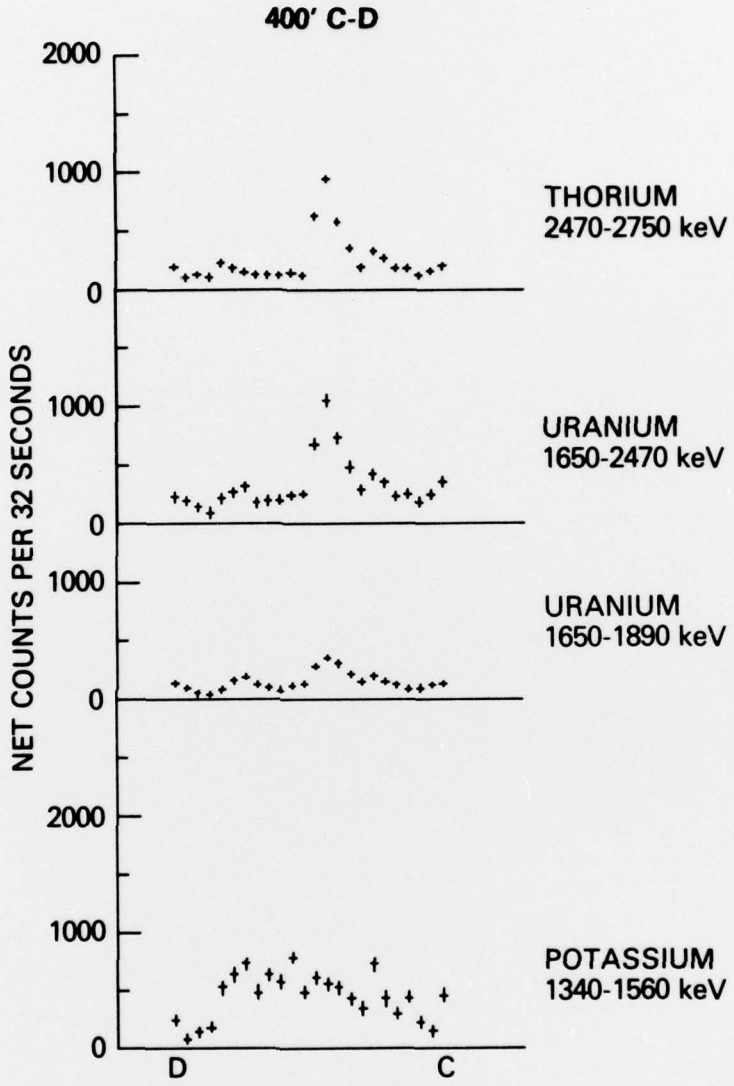

Fig. 15 — NaI(Tℓ) data at 400 ft altitude (C-D) comparing the results for the large and small uranium windows